IOPscience iopscience.iop.org

Home Search Collections Journals About Contact us My IOPscience

Semipolar III–nitride quantum well waveguide photodetector integrated with laser diode for on-chip photonic system

This content has been downloaded from IOPscience. Please scroll down to see the full text.

2017 Appl. Phys. Express 10 042201

(http://iopscience.iop.org/1882-0786/10/4/042201)

View the table of contents for this issue, or go to the journal homepage for more

Download details:

IP Address: 109.171.137.210
This content was downloaded on 07/03/2017 at 06:38

Please note that terms and conditions apply.

You may also be interested in:

Continuous-Wave Operation of Pure Blue AlGaN-Cladding-Free Nonpolar InGaN/GaN Laser Diodes
Kathryn M. Kelchner, Robert M. Farrell, You-Da Lin et al.

A High Power InGaN-Based Blue-Violet Laser Diode Array with a Broad-Area Stripe
Chen Ping, Zhao De-Gang, Feng Mei-Xin et al.

GaN directional couplers for on-chip optical interconnect
Jialei Yuan, Xumin Gao, Yongchao Yang et al.

Materials and growth issues for high-performance nonpolar and semipolar LEDs
R M Farrell, E C Young, F Wu et al.

Room-Temperature Continuous-Wave Operation of InGaN Multi-Quantum-Well Laser Diodes Grown on an n-GaN Substrate with a Backside n-Contact
Masaru Kuramoto, Chiaki Sasaoka, Yukihiro Hisanaga et al.

InGaN based green laser diodes on semipolar GaN substrate
Masahiro Adachi

Improving output power performance of InGaN-based light-emitting diodes by employing step-down indium contents
Daesung Kang, Taejoon Kim, Kiyoung Song et al.

Non-polar and semipolar nitride semiconductors
Jung Han and Michael Kneissl

OPEN ACCESS
Applied Physics Express **10**, 042201 (2017)
https://doi.org/10.7567/APEX.10.042201

Semipolar III–nitride quantum well waveguide photodetector integrated with laser diode for on-chip photonic system

Chao Shen[1], Changmin Lee[2], Edgars Stegenburgs[1], Jorge Holguin Lerma[1], Tien Khee Ng[1], Shuji Nakamura[2], Steven P. DenBaars[2], Ahmed Y. Alyamani[3], Munir M. El-Desouki[3], and Boon S. Ooi[1*]

[1]Photonics Laboratory, King Abdullah University of Science and Technology (KAUST), Thuwal 21534, Saudi Arabia
[2]Materials Department, University of California Santa Barbara (UCSB), Santa Barbara, CA 93106, U.S.A.
[3]King Abdulaziz City for Science and Technology (KACST), Riyadh 11442, Saudi Arabia

*E-mail: boon.ooi@kaust.edu.sa

Received December 19, 2016; accepted February 13, 2017; published online February 28, 2017

A high-performance waveguide photodetector (WPD) integrated with a laser diode (LD) sharing the single InGaN/GaN quantum well active region is demonstrated on a semipolar GaN substrate. The photocurrent of the integrated WPD is effectively tuned by the emitted optical power from the LD. The responsivity ranges from 0.018 to 0.051 A/W with increasing reverse bias from 0 to 10 V. The WPD shows a large 3 dB modulation bandwidth of 230 MHz. The integrated device, being used for power monitoring and on-chip communication, paves the way towards the eventual realization of a III–nitride on-chip photonic system. © 2017 The Japan Society of Applied Physics

Group III–nitride materials, mainly (In,Ga)N, have been mostly studied for active devices, including light-emitting diodes (LEDs),[1,2] superluminescent diodes (SLDs),[3,4] and laser diodes (LDs),[5,6] in the violet–blue–green color regime. Those light emitters based on InGaN/GaN quantum-well (QW) structures have been used in applications for energy-efficient solid-state lighting (SSL)[7,8] and high-speed visible light communication (VLC).[9,10] Additionally, the same structure can be configured for passive devices, serving the functionalities of transverse transmission modulators[11] and surface photodetectors (SPDs).[12] The combination of both active and passive components enables the possible on-chip integration of optoelectronic devices with versatile functionalities.[13] However, the combination of SPDs with surface light emitters, such as LEDs, is not a cost-effective and mass-producible approach owing to the fabrication complexity. Hence, the utilization of edge-emitting laser diodes together with light modulators or receivers based on the same active region becomes a promising approach. The major challenge is the large separation between the absorption and emission peaks, i.e., the Stokes shift, induced by the strong polarization field in conventional *c*-plane-orientated InGaN/GaN QWs.[14] Our recent investigation has shown that this can be addressed by growing active layers on a semipolar GaN substrate, and the waveguide-modulator-integrated laser diode has been demonstrated for SSL–VLC applications.[15] To achieve an LD-based on-chip photonic system, it is of great interest to develop a high-performance waveguide photodetector (WPD) and investigate its integration with laser diodes. In this work, a III–nitride waveguide PD integrated with a laser diode at 405 nm sharing the identical active region on semipolar $(20\bar{2}\bar{1})$ GaN substrate is demonstrated. High responsivities of 0.018 and 0.051 A/W are measured at 0 and −10 V biases, respectively. The WPD shows a large 3 dB modulation bandwidth of ~230 MHz, suggesting its great potential for on-chip power monitoring and communication applications.

The epitaxial structure of the device contains a highly Mg-doped p-GaN contact layer, a 600 nm Mg-doped p-GaN cladding layer, a 120 nm Mg-doped p-InGaN separate confinement heterostructure (SCH) waveguiding layer, a 16 nm Mg-doped p-$Al_{0.18}Ga_{0.82}N$ electron-blocking layer (EBL), a four-period 3.6 nm/7 nm $In_{0.1}Ga_{0.9}N$/GaN multiple-QW active region, a 120 nm Si-doped n-InGaN SCH waveguiding layer, a 350 nm Si-doped n-GaN cladding layer, and a highly Si-doped n-GaN contact layer, as shown in Fig. 1(a). It is grown on a semipolar $(20\bar{2}\bar{1})$–orientated free-standing GaN substrate by metal–organic chemical vapor deposition (MOCVD). The Pd/Au and Ti/Al/Ni/Au metal stacks are deposited as p- and n-GaN contacts, respectively.

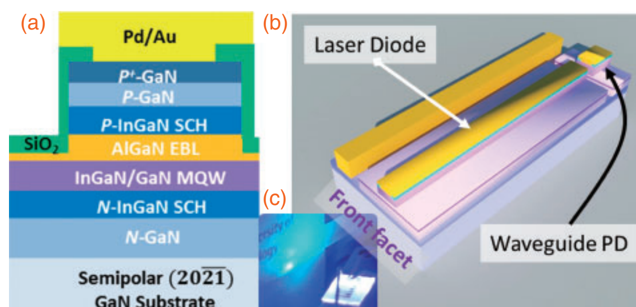

Fig. 1. (a) Epitaxial layer structure, (b) schematic of the InGaN/GaN MQW based WPD-LD, and (c) photo of the laser emission from the front facet of the WPD-LD.

The fabricated WPD-LD shown in Fig. 1(b) consists of a 90-µm-long WPD placed at the rear facet of a 505-µm-long LD, with a separation distance of ~5 µm. The 2-µm-wide ridge waveguide and the facets are defined by UV photolithography and plasma etching, without facet coating. The isolation trench is etched by focused ion beam (FIB) milling. The isolation resistance between the WPD and the LD is measured to be ~1 MΩ, which is more than five orders of magnitude higher than the junction series resistance, enabling the independent operation of the two components.

The LD is characterized using a Keithley 2520 diode laser testing system with a calibrated Si photodetector and an integrating sphere for accurate measurements of the optical power vs current (*L–I*) characteristics. Figure 1(c) shows

Content from this work may be used under the terms of the Creative Commons Attribution 4.0 license. Any further distribution of this work must maintain attribution to the author(s) and the title of the work, journal citation and DOI.

 © 2017 The Japan Society of Applied Physics

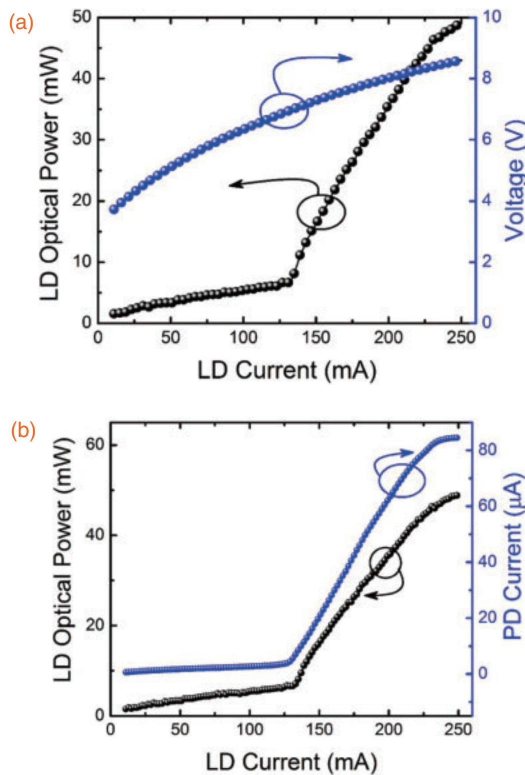

Fig. 2. (a) Plot of light output power collected from the front facet vs current injection and voltage vs current injection relations in the LD. (b) Comparison of LD output power vs current in LD and photocurrent from the WPD at zero bias vs current in LD.

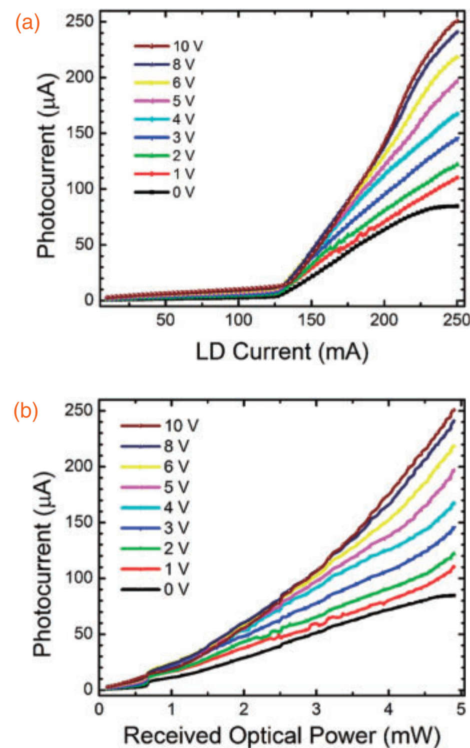

Fig. 3. (a) Measured photocurrent in the WPD as a function of injection current in the LD region under different reverse biases applied to the WPD. (b) Calculated photocurrent as a function of the received optical power in the WPD.

the laser emission from the front facet. The WPD is biased using a Keithley 2400 source meter. The frequency response measurement setup involves an Agilent E8257D analog signal generator, a set of microwave probes, a bias tee, and an Agilent DSO5034A oscilloscope. The LD is modulated by sinusoidal waveform signals at different frequencies, and the received signals from the WPD are collected and analyzed using the oscilloscope.

Figure 2(a) shows the light–current–voltage characteristics of a 405 nm emitting LD under continuous wave (CW) operation, which is measured at the front facet using a standard calibrated Si PD at room temperature. The LD shows a threshold current (I_{th}) of 130 mA and a slope efficiency of ~0.4 W/A. Figure 2(b) compares the LD light output power (collected from the front facet) and the photocurrent from the WPD at zero bias, which is plotted against the LD injection current. It can be observed that the WPD current measured at zero WPD bias is very well correlated with the emitted optical power by the LD. The onset of significant increase in WPD current is measured at an LD current of 130 mA, which matches the threshold current of the LD. With increasing LD injection current beyond I_{th}, the LD starts to lase, and thus more light is received by the WPD, leading to a clear increase in WPD current. Therefore, the integrated WPD can be utilized for on-chip power monitoring.

An enhanced optical responsivity is achieved from the biased WPD as shown in Fig. 3(a). To minimize the heating effect of the LD, the pulsed current operation of the LD with a pulse width of 5 μs and a duty cycle of 10% was used for further characterization of the WPD-LD. With an increasing reverse bias applied to the WPD, the width of the depletion junction in the active region increases, resulting in increased absorption and photocurrent. For instance, at a constant LD current (I_{LD}) of 200 mA, the WPD photocurrents (I_{PD}) are 63.5, 80.7, 112.3, and 130.4 μA, at WPD reverse bias voltages (V_{PD}) of 0, 2, 4, and 6 V, respectively. Figure 3(b) presents the WPD current as a function of the received optical power. The results are derived on the basis of assumptions that the amounts of light emitted from the uncoated front and back facets of the LD are identical, and all the light emitted is received by the WPD. Note also that the reflection of photons on the facet of the WPD is unavoidable and an enhanced photocurrent can be expected by depositing an antireflection (AR) coating on the WPD. In Fig. 3, a clear power-dependent PD response is observed, where the slope of the WPD response curves grows with increasing reverse bias. The enhanced responsivity indicates that the WPD operating in the photoconductive mode is advantageous for weak signal detection. The responsivity (R) can be calculated according to the ratio of I_{PD} over the incident optical power. The measured R vs V_{PD} relation is plotted in Fig. 4. With increasing reverse bias voltage from 0 to 10 V, the R of the WPD increases from 0.018 to 0.051 A/W. With increasing reverse bias applied to the WPD, which operates in the photoconductive mode, the numbers of electrons and holes generated from the junction increase, leading to the enhanced responsivity. Considering the fact that the WPD and LD share the same active layer design without the need of epitaxial regrowth, the presented WPD outperforms other PDs utilizing InGaN/GaN QWs on *c*-plane-orientated substrates (0.001–0.01 A/W at 450 nm) for simultaneous light emission and detection.[13,16–18] The high responsivity of the WPD is attributed to the enhanced overlap between the absorption peak of the WPD and the

© 2017 The Japan Society of Applied Physics

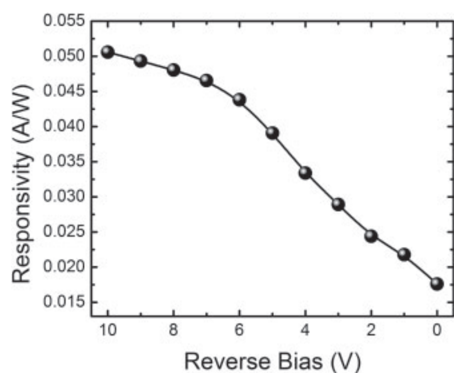

Fig. 4. Measured responsivity as a function of the reverse bias in the waveguide PD.

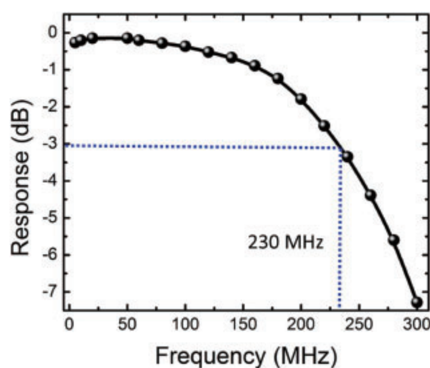

Fig. 5. Modulation response of the waveguide photodetector at zero bias.

emission peak of the LD. The enhancement in the overlap originates from a reduced polarization field in QWs grown on a semipolar GaN substrate.

The frequency response of the unbiased WPD-LD has been measured to study the performance of the device for on-chip communication as shown in Fig. 5. The emitted light from the LD was modulated by the applied small signal and received by the WPD at $V_{PD} = 0$ V. Since the modulation bandwidth of the LD is beyond GHz,[19] the measured signal amplitude decay is thus due to the WPD bandwidth. A 3 dB bandwidth of ∼230 MHz is measured, suggesting a significantly improved modulation performance compared with the reported GaN Schottky barrier PDs (5.4 MHz)[16] and GaN p–i–n PDs (10–20 MHz).[13] The increased cutoff frequency of the WPD is associated with the reduced device size owing to the narrow ridge design and the improved responsivity of the semipolar plane WPDs. The high-speed WPD suggests its potential as an integrated receiver for on-chip communication and VLC applications.

In summary, an integrated waveguide photodetector–laser diode has been designed, fabricated, and demonstrated. Sharing the same InGaN/GaN QW structure, the semipolar plane WPD exhibits a high responsivity of 0.051 A/W at −10 V, 405 nm, and a large modulation bandwidth of 230 MHz. As LDs outperform LEDs in terms of efficiency droop and modulation bandwidth, the LD-based integrated photonic platform becomes more promising for both SSL and VLC applications. Therefore, the presented work of the WPD-LD is an important step towards the eventual realization of a III–nitride on-chip photonic system with integrated functionalities.

Acknowledgments This work was supported by King Abdullah University of Science and Technology (KAUST) baseline funding (BAS/1/1614-01-01), King Abdulaziz City for Science and Technology (KACST) Technology Innovation Center (TIC) for Solid State Lighting (KACST TIC R2-FP-008), and KACST-KAUST-UCSB Solid-State Lighting Program.

1) S. Nakamura, M. Senoh, N. Iwasa, and S. Nagahama, Jpn. J. Appl. Phys. **34**, L797 (1995).
2) C. C. Pan, S. Tanaka, F. Wu, Y. Zhao, J. S. Speck, S. Nakamura, S. P. DenBaars, and D. Feezell, Appl. Phys. Express **5**, 062103 (2012).
3) C. Shen, T. K. Ng, J. T. Leonard, A. Pourhashemi, S. Nakamura, S. P. DenBaars, J. S. Speck, A. Y. Alyamani, M. M. El-Desouki, and B. S. Ooi, Opt. Lett. **41**, 2608 (2016).
4) C. Shen, C. Lee, T. K. Ng, S. Nakamura, J. S. Speck, S. P. DenBaars, A. Y. Alyamani, M. M. El-Desouki, and B. S. Ooi, Opt. Express **24**, 20281 (2016).
5) M. T. Hardy, D. F. Feezell, S. P. DenBaars, and S. Nakamura, Mater. Today **14**, 408 (2011).
6) S. Izumi, N. Fuutagawa, T. Hamaguchi, M. Murayama, M. Kuramoto, and H. Narui, Appl. Phys. Express **8**, 062702 (2015).
7) S. Nakamura, MRS Bull. **34**, 101 (2009).
8) M. Cantore, N. Pfaff, R. M. Farrell, J. S. Speck, S. Nakamura, and S. P. DenBaars, Opt. Express **24**, A215 (2016).
9) H. Chun, P. Manousiadis, S. Rajbhandari, D. A. Vithanage, G. Faulkner, D. Tsonev, J. J. D. McKendry, S. Videv, E. Y. Xie, E. D. Gu, M. D. Dawson, H. Haas, G. A. Turnbull, I. D. W. Samuel, and D. C. O'Brien, IEEE Photonics Technol. Lett. **26**, 2035 (2014).
10) C. Lee, C. Shen, H. M. Oubei, M. Cantore, B. Janjua, T. K. Ng, R. M. Farrell, M. M. El-Desouki, J. S. Speck, S. Nakamura, B. S. Ooi, and S. P. DenBaars, Opt. Express **23**, 29779 (2015).
11) E. Sari, S. Nizamoglu, T. Ozel, and H. V. Demir, Appl. Phys. Lett. **90**, 011101 (2007).
12) Y. T. Huang, P. H. S. Yeh, Y. H. Huang, Y. T. Chen, C. W. Huang, C. J. Lin, and W. C. Yeh, IEEE Photonics Technol. Lett. **28**, 605 (2016).
13) W. Cai, X. M. Gao, W. Yuan, Y. C. Yang, J. L. Yuan, H. B. Zhu, and Y. J. Wang, Appl. Phys. Express **9**, 052204 (2016).
14) Y. Zhang, R. M. Smith, Y. Hou, B. Xu, Y. Gong, J. Bai, and T. Wang, Appl. Phys. Lett. **108**, 031108 (2016).
15) C. Shen, T. K. Ng, J. T. Leonard, A. Pourhashemi, H. M. Oubei, M. S. Alias, S. Nakamura, S. P. DenBaars, J. S. Speck, A. Y. Alyamani, M. M. Eldesouki, and B. S. Ooi, ACS Photonics **3**, 262 (2016).
16) Z. Y. Jiang, M. R. M. Atalla, G. J. You, L. Wang, X. Y. Li, J. Liu, A. M. Elahi, L. Wei, and J. Xu, Opt. Lett. **39**, 5657 (2014).
17) J. Pereiro, C. Rivera, A. Navarro, E. Munoz, R. Czernecki, S. Grzanka, and M. Leszczynski, IEEE J. Quantum Electron. **45**, 617 (2009).
18) Y. D. Jhou, C. H. Chen, R. W. Chuang, S. J. Chang, Y. K. Su, P. C. Chang, P. C. Chen, H. Hung, S. M. Wang, and C. L. Yu, Solid-State Electron. **49**, 1347 (2005).
19) C. Lee, C. Zhang, D. L. Becerra, S. Lee, C. A. Forman, S. H. Oh, R. M. Farrell, J. S. Speck, S. Nakamura, J. E. Bowers, and S. P. DenBaars, Appl. Phys. Lett. **109**, 101104 (2016).

© 2017 The Japan Society of Applied Physics